Fostered Thermomagnetic Stabilities and Boosted Mechanical Reliability Related to High Trapped Field in Composite Bulk YBa2Cu3O7−δ Cryomagnets

ARTICLE *in* JOURNAL OF PHYSICAL CHEMISTRY LETTERS · JULY 2015

Impact Factor: 7.46 · DOI: 10.1021/acs.jpclett.5b00906

6 AUTHORS, INCLUDING:

Driss Kenfaui

French National Centre for Scientific Research

23 PUBLICATIONS **188** CITATIONS

SEE PROFILE

Gomina Moussa

National Graduate School of Engineering and …

218 PUBLICATIONS **868** CITATIONS

SEE PROFILE

Eric Louradour

Céramiques Techniques Industrielles

16 PUBLICATIONS **37** CITATIONS

SEE PROFILE

THE JOURNAL OF PHYSICAL CHEMISTRY Letters

Letter

pubs.acs.org/JPCL

Fostered Thermomagnetic Stabilities and Boosted Mechanical Reliability Related to High Trapped Field in Composite Bulk $YBa_2Cu_3O_{7-\delta}$ Cryomagnets

Driss Kenfaui,*[,†] Pierre-Frédéric Sibeud,[†] Moussa Gomina,[§] Eric Louradour,[∥] Xavier Chaud,[‡] and Jacques G. Noudem[§]

[†]CNRS/CRETA, B.P. 166, 38042 Grenoble Cedex 09, France

[‡]CNRS/LNCMI, UPS-INSA-UJF, B.P. 166, 38042 Grenoble Cedex 09, France

[§]CRISMAT/LUSAC, UMR 6508 ENSICAEN/CNRS, Université Caen Basse-Normandie, 6 Bd Maréchal Juin, 14050 Caen Cedex 04, France

[∥]CTI SA, 382 du Moulinas-La Resclause, 30340 Salindres, France

ABSTRACT: In the quest of $YBa_2Cu_3O_{7-\delta}$ (Y123) bulk superconductors providing strong magnetic fields without failure, it is of paramount importance to achieve high thermal stabilities to safeguard the magnetic energy inside them during the trapping-field process, and sufficient mechanical reliability to withstand the stresses derived from the Lorenz force. Herein, we experimentally demonstrate a temperature rise induced by dissipative flux motion inside an Y123 thin-wall superconductor, and a significant thermal exchange in a composite bulk Y123 cryomagnet realized by embedding this superconductor with high thermal-conductivity metal network. It resulted in stimulating the maximum trapped field B_m, which reached 6.46 T on 15.9 mm-diameter single disk superconductor after magnetization by field cooling to 17 K under 7 T, leading to an improvement of 18% compared to the thin-wall superconductor. The composite cryomagnet particularly revealed the potential to trap stronger fields if larger magnetic activation is available. By virtue of the pore-free and crack-free microstructure of this cryomagnet, its strength σ_R was estimated to be 363 MPa, the largest one obtained so far for Y123 bulk superconductors, thus suggesting a striking mechanical reliability that seems to be sufficient to sustain stresses derived from trapped fields stronger than any values hitherto reported.

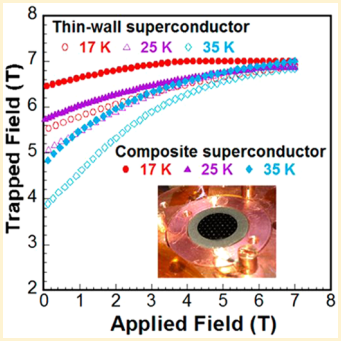

Rare-earth (RE)−Ba−Cu−O bulk superconductors cooled below their critical temperature under a magnetic activation are typified by the ability to trap a part or almost all the applied field, thereby providing a viable route for producing magnetic fields substantially larger than those achievable with conventional permanent Nd−Fe−B magnets.[1−9] They offer the possibility of generating portable high fields outside the bore of superconducting solenoids, and can thus be used as a new class of permanent magnets better known as cryomagnets,[4] potentially desirable for practical engineering applications such as frictionless bearings, superconducting motors, flywheel energy storage, magnetic separation systems, and magnetron sputtering devices.[4,10] The trapped field takes its origin from the persistent currents macroscopically flowing in a (RE)−Ba−Cu−O bulk superconductor and presents a spatial distribution on the sample surface with the main features of a maximum trapped field B_m at the center and a field gradient toward the edge.[11] The B_m magnitude is hence dictated not only by the critical current density J_c, which can be furthered by introducing effective pinning sites into the material,[4,8,9] but also by the size of the persistent current loops, which can be increased by elaborating large single-grain superconductors possessing a pore-free and crack-free microstructure.[2,12]

Strong volume pinning forces were achieved in bulk $YBa_2Cu_3O_{7-\delta}$ (Y123) superconductors by zinc-doping the precursors before the crystal growth of samples in the form of large single grains, communally called single domains.[4,8,9] It resulted in high J_c densities enabling to reach a trapped field larger than 11 T at 17 K on a 26 mm-diameter zinc-doped Y123 single pellet, which was mechanically reinforced prior to the trapping process to deal with the imparted magnetic stresses.[9] Yet, the sizes of the current loops are considerably reduced in such traditional plain Y123 superconductors as a consequence of both pores, stemmed from the entrapment of oxygen gas bubbles upon the solidification during the crystal processing,[13] and an intensive cracks network[4,7] occurring in the grown grain when being annealed at 400−500 °C under 0.1 MPa oxygen flow (conventional oxygenation) to recover its superconducting properties by reducing the oxygen deficit[14] $\delta < 0.2$.

Accordingly, we have recently reported the fabrication of pore-free and crack-free Y123 bulk superconductors endowed with high trapped field performances arising from large size nondeformed current loops circulating in the (a,b) planes of

Received: May 2, 2015
Accepted: July 15, 2015

DOI: 10.1021/acs.jpclett.5b00906
J. Phys. Chem. Lett. 2015, 6, 2999−3005

the samples.[2,12] Briefly, the top-seeded melt growth (TSMG) process[15,16] was used to grow large thin-wall Y123 single domains from {70 wt % Y123, 30 wt % Y_2BaCuO_5 (Y211) and 0.15 wt % PtO_2 (in excess)} precursors previously compacted into drilled preforms comprising a high number of holes spaced by thin walls.[4,12] The preforms were primarily heated in air up to 1054 °C and held for 2 h to get a peritectic decomposition into a solute rich in barium and copper, and skeleton of solid Y211 inclusions. The large amount of oxygen, released in the form of gas bubbles at such elevated temperature, crossed more readily thin walls of the preforms to escape through the large specific areas provided by the holes network than a diameter of traditional plain pellets. It resulted hence in the avoidance of the oxygen bubbles entrapment during the crystal growth and, subsequently, in pore-free microstructure. The crystal growth was oriented by a commercial 2 × 2 mm^2 seed, NdBCO thin layer deposited on MgO substrate (Theva Gmbh films),[17,18] placed on the upper surface of the precursor prior to TSMG processing.

To capitalize on merits of reduced diffusion paths and large specific areas allowed by the thin-wall Y123 single domains, the latters were progressively annealed[19] under oxygen pressure up to 10 MPa at a temperature as high as 700 °C. Here, the purpose was to speed up the oxygen diffusion, which is reported to display very low rates in the Y123 crystal under the classical oxygenation conditions,[20,21] 10^{-7} cm^2 s^{-1} in the (a,b) planes and much slower along the *c*-axis. The stresses, induced by the oxygen gradients tied to such oxygen diffusion, were thus maintained below the material strength σ_R during the tetragonal to orthorhombic transition and cell c-parameter shortening regularly occurring in the Y123 material when being cooled from 900 °C to room temperature.[14] It resulted in realizing thin-wall Y123 single domains possessing a crack-free microstructure.[2] Note that the c-parameter contracts over a very short crystal depth in the case of traditional plain Y123 pellets classically oxygenated because of the very low oxygen diffusion. The external oxygenated layers are consequently under a high tensile stresses since the crystal core is still less oxygenated with the larger primitive c-parameter. These stresses reach a level above the material strength σ_R (<30 MPa)[22] severely impaired by the high porosity, thus causing microstructure cracking.

On the flip side, the B_m magnitude is strongly dependent on the Y123 superconductor temperature in the ≤92 K range.[4,6−9] The lower the temperature, the larger the B_m magnitude. Hence, the weak thermal exchange inside the Y123 crystal assigned to its very low anisotropic thermal conductivity, 14 $W \cdot m^{-1} K^{-1}$ in the (a,b) planes and 4-fold lower along the *c*-axis,[4,7] complicates efforts to boost the trapped fields. Indeed, the heat generated in the Y123 bulk sample during the trapping-field process cannot be immediately dissipated, which arises the temperature inside the superconductor, thereby impairing the trapping properties or, even, causing a sudden thermal instability, as flux jumping, and, consequently, a catastrophic quenching of the bulk superconductor leading to the suppression of trapped field and irreversible material damage.[4,6−9]

Here we experimentally demonstrate a temperature rise inside the Y123 thin-wall superconductors during the field-trapping process although their larger specific areas compared to the traditional plain Y123 materials, and an effective dissipation of the heat generated during this process inside a composite bulk Y123 superconductor achieved by embedding the holes of the thin-wall sample with a network of high thermal-conductivity metal wires. Such heat dissipation is essential for the achievement of thermomagnetic stabilities required for avoiding flux jumping, and subsequently safeguarding the trapped field. By developing a practical experimental setup for magnetizing and rapidly refrigerating the bulk Y123 material to operating temperatures well below 77 K, the trapped field capabilities of this composite cryomagnet were extensively studied and compared to the largest ones reported so far in thin-wall and traditional plain Y123 single domains. Its strength was likewise estimated, which enabled to estimate the largest field that it can trap without failure.

Thin-Wall $YBa_2Cu_3O_{7-\delta}$ Bulk Superconductor. Large thin-wall single domain, comprising 55 holes ordered in a regular hexagonal network (Figure 1, left), was grown using TSMG process and then progressively annealed under the aforementioned temperature and oxygen pressure for 12 h (ref 2). The holes network did not impede the crystal growth nor was destroyed upon TSMG processing, but the material depicted a macroscopic shrinking evidenced by a reduction of the pellet diameter from 20 to 15.9 ± 0.2 mm. The diameter of seven large holes, previously introduced around the perimeter and at the center of the disk pellet, was consequently curtailed from 0.7 to 0.57 ± 0.02 mm and that of forty-eight other small ones from 0.5 to 0.43 ± 0.03 mm (Figure 1, right) after the crystal growth. The walls thickness between small holes was contracted from 2.10 to 1.60 ± 0.10 mm, and that between large holes and their immediate small-hole neighbors from 1.92 to 1.50 ± 0.07 mm.

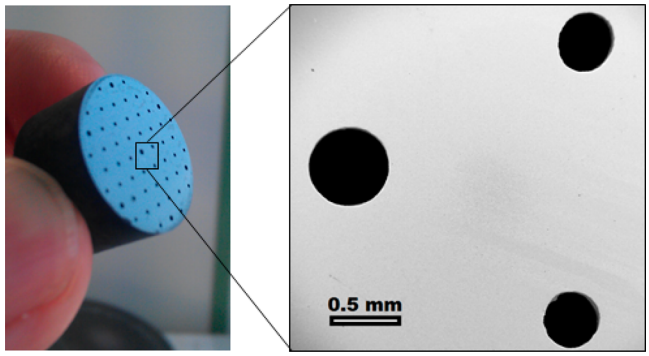

Figure 1. (left) Large thin-wall single domain, comprising 55 holes ordered in a regular hexagonal network, grown using the TSMG process from {70 wt % Y123, 30 wt % Y211 and 0.15 wt % PtO_2 (in excess)} precursors previously compacted into drilled preform. (right) The diameters of large and small holes are 0.57 ± 0.2 and 0.43 ± 0.03 mm upon the TSMG process, while the walls thickness between small holes and that between large holes and their immediate small-hole neighbors are 1.60 ± 0.10 and 1.5 ± 0.07 mm, respectively.

Scanning electron microscopy (SEM) observations, performed on a mirror-polished surface (Figure 2) cut from the core of the sample in the direction parallel to the *c*-axis, showed a Y123 matrix, in bright contrast, including evenly distributed Y211 particles categorized into two types of size: small majority inclusions (1−4 μm) and large minority particles (<20 μm). Such size appears to be larger than that reported elsewhere,[19] probably due to the Y211 precursor since the sample was fabricated using the same method. The observations particularly evidenced a pore-free and crack-free microstructure of the thin-wall superconductor as a result of both no entrapment of oxygen gas bubbles upon the material solidification, and the fact that the stresses, induced by the oxygen gradients, were

DOI: 10.1021/acs.jpclett.5b00906
J. Phys. Chem. Lett. 2015, 6, 2999−3005

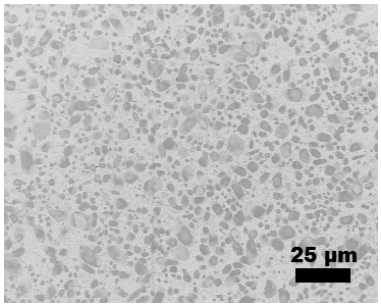

Figure 2. SEM micrograph of mirror-polished surface cut parallel to the vertical *c*-axis of the single domain progressively oxygenated at 700 °C under 10 MPa for 12 h: Y123 matrix, in bright contrast, comprises small majority Y211 inclusions (1−4 μm) and large minority Y211 particles (<20 μm). One particularly notes the absence of pores and cracks in the achieved microstructure.

maintained below the crystal strength σ_R during the progressive annealing thanks to speeding up the oxygen diffusion in the Y123 thin-wall single domain.

The processed thin-wall superconductor was then polished on its two faces (Figure 1) and characterized by measuring the trapped filed spatial distribution at 77 K, by cooling it with liquid nitrogen in an applied field of 1.5 T. After switching off this activation, a scan with an axial Hall sensor was carried out over the upper surface of the sample at a constant sensor-surface distance of 0.2 mm. The results showed a single homogeneous peak culminating at 475 mT.

Magnetization and Rapid Refrigeration to Operating Temperatures. Most importantly, a great deal of effort was put into developing a practical experimental setup well-suited for magnetizing and rapidly refrigerating the bulk superconductor to operating temperatures well below 77 K. Briefly, this system is made up of a sample stage cooled by the instrumented Cryomech AL230 cryocooler in a cryostat placed in an Oxford superconducting coil generating a magnetic field up to 7 T. The sample stage is a copper support (Figure 3a,b) designed to effectively sink the heat to be extracted from the bulk Y123 material during the field-trapping process. The cryogenic refrigeration, based on closed-loop pure helium expansion cycles, is achieved by the mean of two major components of the cryocooler device: (i) the compressor package, which compresses refrigerant (helium) and extracts heat from the system, and (ii) the cold head, which takes refrigerant through expansion cycles to cool it down to cryogenic temperatures. Steel lines carry compressed helium from the compressor to the cold head and carry low-pressure helium back.

Achieving low cryogenic temperatures, moreover, requires a significant reduction of radiant, convection, and/or conduction heating around the clod head/sample stage arrangement. For that purpose, we wrapped the latter in several superinsulation film layers (Jehier SA - Hutchinson Group, France) to limit radiant heating on the one hand, and created a vacuum up to 10^{-5} mbar in the cryostat to suppress convection on the other hand. The chemical composition as well as the size of the metallic wires, used to connect the probes or the resistive heater to the control and measuring devices, were taken into account with a view to minimize the conduction heating arising from the heat dissipated by the Joule effect and the heat transfer from the hot side to the cold one of the wires located, respectively, outside and inside the cryostat.

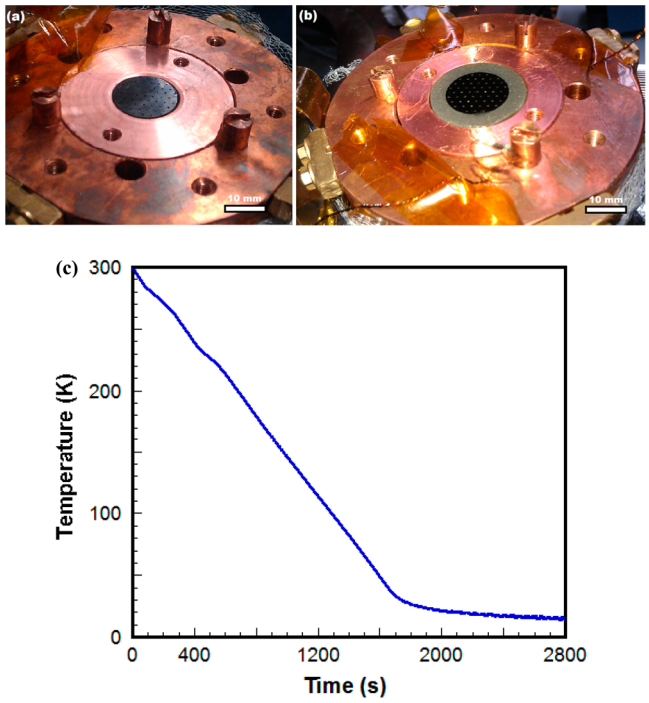

Figure 3. (a) Y123 thin-wall and (b) composite superconductors placed in the stage sample (copper support) designed to effectively sink the heat that will be extracted from them during the field-trapping process. (c) Temperature versus time curve recorded on a Y123 bulk superconductor showing cooling down to temperatures below 20 K in only 30 min by the instrumented Cryomech AL230 cryocooler wrapped with several superinsulation film layers in a cryostat under a vacuum of 10^{-5} mBar.

As a result, Y123 bulk samples were cooled down to temperatures below 20 K in only 30 min as can be seen in Figure 3c, which brings valid and practical solutions to bulk superconductors cooling in terms of the time as well as the cost, thus breaking down one of the key barriers against wide-scale use of the bulk superconductors as a source of strong magnetic fields for engineering applications.

Note that such system was used to calibrate Hall and Cernox sensors in temperature and field ranges as well (0−7 T/11−100 K).

A calibrated Hall sensor was located at the center on the upper surface of the sample placed in the copper support (Figure 3a,b). The temperature of the sample was monitored using a calibrated Cernox sensor put in the vicinity of the Hall one. To deal with the Lorentz force induced by the magnetic field, the superconductor was mechanically fixed, which allowed at the same time to improve remarkably the thermal contacts in the copper support/sample/probes interfaces.

For all the samples, the trapped-field measuring strategy was defined as follows: the sample was first cooled to 100 K and maintained at this temperature, that is, above the critical one of Y123 superconductor (a); the desired external magnetizing field was thus applied at 100 K (b), after which the sample was cooled to the measuring temperature (c). The external field was finally ramped down to zero (d). After field trapping, the sample was warmed up to >92 K to suppress the remanent field (e).

Dissipative Flux Motion in the Thin-wall $YBa_2Cu_3O_{7-\delta}$ Bulk Superconductor. During the latter two steps (d and e) of the measuring strategy, a rapid rise in temperature inside the

DOI: 10.1021/acs.jpclett.5b00906
J. Phys. Chem. Lett. 2015, 6, 2999−3005

sample may occur if either the applied field is decreased or the sample warming performed at uncontrolled rates, which would induce flux jumps, leading to a catastrophic quenching of the bulk superconductor at relatively high rates. To experimentally demonstrate such thermomagnetic phenomena, the thin-wall sample was initially magnetized by field cooling to a measuring temperature of 17 K under 6 T. The applied field was then removed at a sweep rate of 0.1 T·min^{-1} [refs 3, 4, 6−9]. The sample, however, was heated at a low rate of 0.5 K·min^{-1} [refs 2, 4, 6, 8, 9], and at larger one of 2.5 K·min^{-1} in a second separate identical test, during the last step of the measuring strategy (e). Figure 4 shows the temperature dependence of the

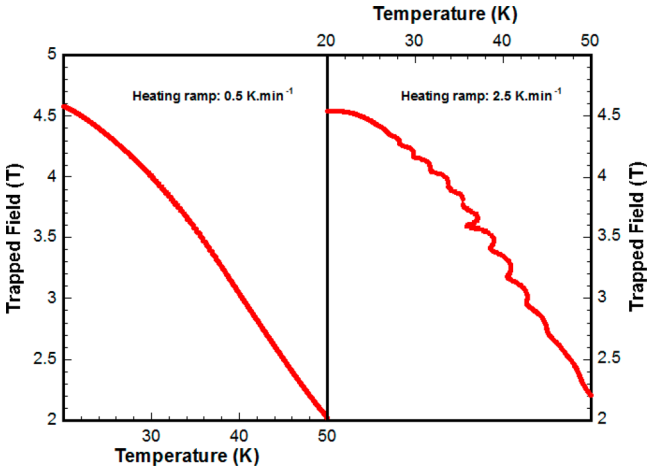

Figure 4. Temperature dependence of the maximum trapped field B_m obtained during heating in the 20−50 K range on the thin-wall superconductor initially magnetized by field cooling to a measuring temperature of 17 K under 6 T. The curves $B_m(T)$ recorded at (left) a low rate of 0.5 K.min^{-1}, and (right) at a larger one of 2.5 K·min^{-1} in a second separate identical test.

maximum trapped field B_m measured on the top of the sample at each rate in the 20−50 K range. The $B_m(T)$ curve recorded at 2.5 K·min^{-1} evidenced undershoot/overshoot behavior compared to the one obtained at 0.5 K·min^{-1}, which is likely the fingerprint of a temperature elevation inside the sample. Warming at large rate, indeed, causes steeper motion of larger flux lines immediately after being released from their pinning sites as a result of exceeding the present critical current density J_c under the effect of heating. Such flux motion is accompanied by heat dissipation before a rapid redistribution of flux lines, hence of the current loops associated with them, thereby inducing a change in the trapped field. Warming rates higher than 2.5 K·min^{-1} will cause a greater amount of heat, which would be at risk of appearing sudden flux jumping causing material failure.

Thermomagnetic Stabilities in the Composite Bulk $YBa_2Cu_3O_{7-\delta}$ Cryomagnet. The thin-wall superconductor was then embedded by much larger thermal conductivity (~4530 W·m^{-1}·K^{-1} at 17 K) aluminum (Al) wires,[23] with 0.3−0.5 mm in diameter, inserted into its entire holes network. Before that, Apiezon N thermal grease was applied on the Al wires with the purpose of ensuring a good thermal contact between them and Y123 crystal.

A resin loaded with Al metal inclusions was thereafter used to impregnate the sample in vacuum to avoid any formation of the oxygen gas microvoids into the resin.[7] The Al inclusions have an expansion coefficient (2.3×10^{-5}·K^{-1}) closer to that of Y123 (1×10^{-5}·K^{-1}) (ref 7) than that of the resin (($3-4) \times 10^{-5}$·K^{-1}), which can prevent irreversible damage in the resin during the cooling cycles. The Al inclusions were used to improve the thermal conductivity of the resin/inclusions mixture as well.

The achieved composite bulk Y123 superconductor was mirror-polished on its two faces to remove the surface resin and then placed in a high thermal-conductivity copper support as seen from Figure 3b. It was then magnetized by field cooling to different measuring temperatures (35, 25, and 17 K) under 7 T; each temperature was selected during a separate equivalent test. The trapped field was recorded while the applied field was ramped down to zero at a rate of 0.1 T·min^{-1}. We compare in Figure 5a the fields B_m trapped by the composite super-

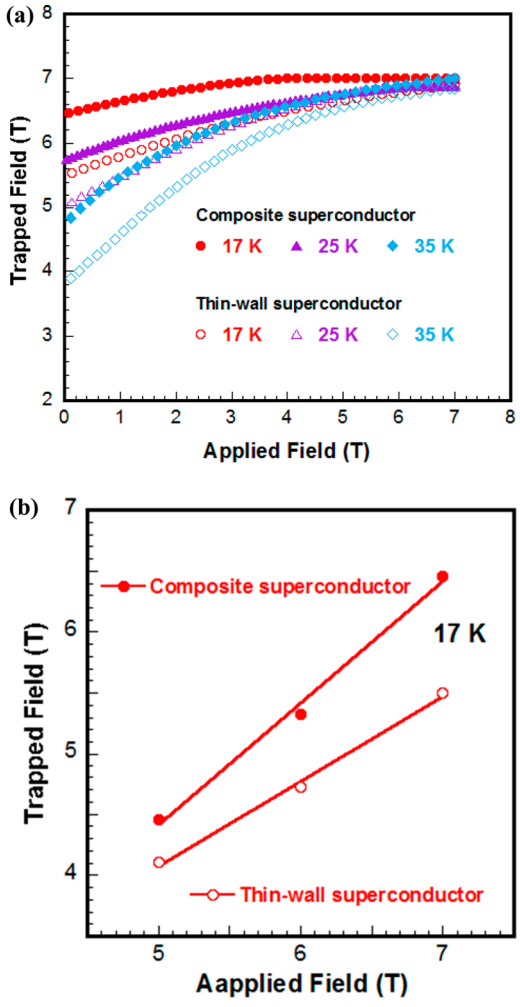

Figure 5. (a) Maximum trapped field B_m measured on the thin-wall and composite superconductors at selected measuring temperatures of 35, 25, and 17 K as the magnetizing field was ramped down to zero. (b) The maximum trapped field B_m measured for both superconductors at 17 K versus the nominal magnetizing field.

conductor during the magnetizing process to those measured on the thin-wall sample in equivalent experiments. The B_m magnitude was found to be markedly larger for the composite superconductor whatever the measuring temperature, which suggests that the magnetic energy stored in such superconductor was much more safeguarded. The high thermal-conductivity Al wires, in fact, enabled to effectively sink the heat amount arising from dissipative flux motion by instantly

DOI: 10.1021/acs.jpclett.5b00906
J. Phys. Chem. Lett. 2015, 6, 2999−3005

extracting it from the bulk material and thus transferring it to the copper support.

It is relevant to note here that given that the Al wires are evenly distributed inside the composite superconductor, they extracted the heat from all its internal regions, thus promoting much higher thermal stability compared to the reinforced Y123 bulk superconductor reported by Tomita et Murakami,[7] wherein only one metal wire was inserted into the center as a heat sink.

Such thermal stability, on the other hand, is concomitantly achieved with the superconductor encapsulating in resin loaded in Al inclusions, which induced compressive stresses during cooling as a result of the superior thermal expansion of the resin over that in the (a,b) plane Y123 bulk material. These stresses compensate for the tensile ones derived from the Lorenz force.[4,6−9]

As a result, the composite superconductor trapped a field B_m = 4.76 at 35 K close to that noted on the thin-wall sample at 25 K, and 5.74 at 25 K larger than the B_m value recorded on the latter at 17 K, evidencing that the heat dissipation shifted the trapped field toward higher temperatures.

A trapped field B_m of 6.46 T was reached at 17 K on such a composite bulk cryomagnet consisting of only a 15.9 mm-diameter pellet superconductor, thus guaranteeing a high density of permanent currents circulating inside it, which is indicative of very strong volume pinning forces, although zinc-doping was not used. The B_m value corresponds to an improvement of 18% compared to the thin-wall superconductor, and leads to a marked field density (B_m/s) = 3.25 T·cm^{-2} (s = 1.984 cm^2 is the disk area of the superconductor), which is the largest value obtained so far for Y123 single samples, including doped and/or reinforced ones magnetized by field cooling to any reported measuring temperature under much stronger fields up to 18 T (refs 2, 4, 6, 8, 9).

These results, furthermore, shed light on the fact that, even when the field magnetizing was ramped down to zero at the reported controlled low rate in the case of the thin-wall superconductor, there was a temperature elevation arising from the heat induced by flux motion. Such heat, in fact, could not be immediately dissipated through the large specific areas provided by the thin-wall sample due to the vacuum applied into the cryostat, which is the same in the holes of the latter. This is why the trapped field for the thin-wall superconductor is limited to less than possible.

Before these experiments, both composite and thin-wall superconductors underwent two equivalent separate tests, where they were magnetized by field cooling to a measuring temperature of 17 K under 6 and 5 T. In Figure 5b, depicted is the trapped field B_m measured at 17 K versus the nominal applied magnetizing field. The composite superconductor exhibited a sharper B_m enhancement compared to the thin-wall one, revealing that such a cryomagnet has the potential to trap much larger fields if stronger magnetizing fields were available for activation.

However, the B_m magnitude was observed to slowly decay with time during the tests presented in Figure 5. After being magnetized by field cooling to 25 K under 7 T, the trapped field B_m was recorded on the composite superconductor for a period of about 15 h after the entire removal of the external magnetizing field as shown in Figure 6. Here, the B_m decay is assigned to the magnetic flux creep,[24] an effect explained by a spontaneous thermal activation of magnetic flux lines out of their pinning sites. That proceeds at a rate proportional to

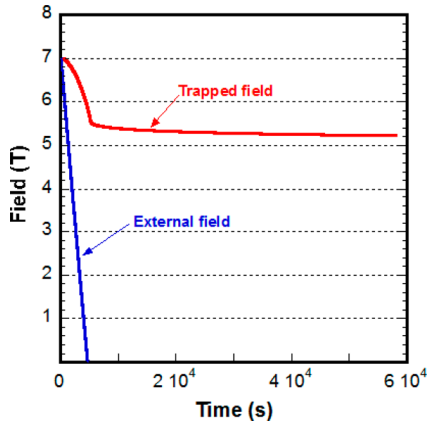

Figure 6. Maximum trapped field B_m recorded on the composite superconductor at 25 K for a long period of about 15 h after the entire removal of the external magnetizing field. We can see a B_m decay with time under the effect of the magnetic flux creep.

$\exp(-U/kT)$, where U is the activation energy, k is Boltzmann's constant, and T is the absolute temperature. This process provokes a redistribution of flux lines, hence of current loops tied to the flux lines, thereby causing a decrease in the B_m magnitude with time. It is therefore clear that such magnetic relaxation is at risk of having a destructive effect with regard to the aforementioned applications.

To cope with such relaxation, we rapidly decreased the measuring temperature of the composite superconductor from 25 to 20 K immediately after removing the external field during an equivalent separate test, and then monitored the trapped field B_m for more than 16 h (Figure 7). We note that the flux creep was suppressed, which can be explained by the fact that the activation energy U increases as the current density J decreases compared to J_c. When the external field was canceled at 25 K, the B_m magnitude was proportional to the critical current density $J \sim J_c$ (at 25 K). The flux profile was hence frozen because of $J < J_c$ (at 20 K), which resulted in safeguarding the trapped field B_m in time.

Mechanical Strength. In addition to their marked trapped field performances, the superconductors achieved here exhibited a high mechanical reliability attributed to their pore-free and crack-free microstructure. Indeed, by introducing microcracking around the indent impressions carried out by Vickers indentation tests on the (a,b) and (a,c)/(b,c) planes, the mean fracture toughness, K_{Ic}, assessed from the applied load and the induced crack lengths according to the formula reported elsewhere,[25,26] exhibited the largest values (2.88 ± 0.09 and 3.1 ± 0.21 MPa·m$^{1/2}$, respectively) reported thus far for the Y123 materials,[4] including those with added Ag doping but excepting the value published for Y123 single domains reinforced with added Ag 2 μm particules.[4,27]

Hence, the fracture toughness in the (a,b) planes determines the maximum tensile stress that our Y123 superconductors can withstand during the field trapping process. It depends otherwise on the material strength σ_R and the size a_0 of the largest defect in the sample through the Irwin equation for brittle fracture:[28] $K_{Ic} = \sigma_R \sqrt{a_0}$, where β is a dimensionless geometrical term that depends on the relative dimensions of the critical defect and the loading geometry and configuration. Since the microstructure is free of pores and cracks (Figure 2) on one hand, and due to the brittle nature of the Y123 material on the other, the rupture will be more likely to occur by a

DOI: 10.1021/acs.jpclett.5b00906
J. Phys. Chem. Lett. 2015, 6, 2999−3005

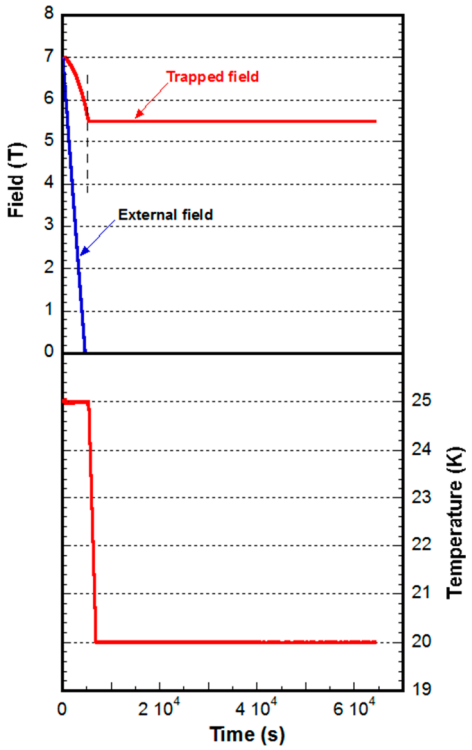

Figure 7. Maximum trapped field B_m monitored on the composite superconductor at 25 K. (bottom) The temperature was then rapidly decreased from the measuring one to 20 K immediately after removing the external field, and (top) B_m recorded for a long period of more than 16 h where the flux creep effect was suppressed.

catastrophic propagation of cracks initiated at the interface between the Y123 matrix and the largest Y211 particle (Figure 2) when the tensile stress induced by the Lorenz force attains the material strength. Therefore, in the worst case, the size of the critical defect in our samples approximates that of the largest Y211 particle, i.e. 20 μm, and hence the β value is $\sqrt{\pi}$. The estimated strength σ_R was then of ~363 MPa, representing an enhancement by a factor of 2.7 compared to the largest σ_R value reported hitherto for Y123 with added Ag particles.[4,27]

The material strength σ_R, on the other hand, sets the maximum trapped field B_m via the formula: $\sigma_R = 0.282\ B_m^2$ (refs 7, 29), where σ_R is in MPa and B_m is in T. The largest trapped field B_m that our superconductors can sustain before failure was then estimated to be of a value as high as 35.8 T, which is larger than all those reported up to date.[3,4,6−9] Note that this result does not guarantee that our cryomagnet has the ability to trap such a strong B_m value, but indicates rather that the superconductor seems to possess the mechanical reliability that could sustain the stresses deriving from such a maximum trapped field B_m. To achieve B_{max} values close to the estimated one, others factors that also govern the trapped field capabilities have to be concomitantly and sufficiently improved, essentially the pining sites density which was not investigated here.

Finally, we conclude that high thermomagnetic stabilities concomitant with a high reliability so-long sought for trapping strong fields could be achieved in composite bulk cryomagnet fabricated by embedding a high thermal-conductivity metal network in a thin-wall superconductor possessing a pore-free and crack-free microstructure. We demonstrated that flux creep effect was suppressed in such cryomagnet, thus enabling to trap strong magnetic field for long period without decay in time. A field B_m of 6.46 T was trapped at 17 K leading to the largest field density (B_m/s) = 3.25 T·cm^{-2} attained hitherto for Y123 bulk superconductors. The composite cryomagnet showed, in particular, the potential to trap much larger static fields for higher activations, and an estimated strength, the largest one achieved so far in Y123 bulk materials, which endowed it with the high mechanical reliability required for trapping magnetic fields larger than all the trapped fields reported up to date.

It emerges from the results reported here that composite cryomagnets turn out to address the major challenges facing the development of Y123 bulk superconductors, which will make them much more well-suited for potential applications, thus opening the door for a large-scale use of rare-earth (RE)−Ba−Cu−O bulk superconductors.

AUTHOR INFORMATION

Corresponding Author

*Address: IJL/CNRS UMR 7198 CNRS - Université Lorraine Parc de Saurupt, CS 50840 54011 Nancy Cedex - France. E-mail: driss.kenfaui@univ-lorraine.fr; Tel. (33) 6 59 30 28 92.

Notes

The authors declare no competing financial interest.

ACKNOWLEDGMENTS

We thank Prof. Daniel Chateigner, Dr. Daniel Bourgault and PhD student Simeon Nachev for the fruitful discussions on Y123 crystal characteristics as well as on trapping and thermal properties, and Dr. Alain Ravex for the sound advice on cryogenics. This work is supported by the French National Research Agency (Agence Nationale de la Recherche - ANR) via both grants ANR-09-MAPR-002 (ASPAMEX Project) and ANR-2010-BLAN-0944-02 (REIMS project).

REFERENCES

(1) Grissonnanche, G.; Cyr-Choinière, O.; Laliberté, F.; René de Cotret, S.; Juneau-Fecteau, A.; Dufour-Beauséjour, S.; Delage, M.-E.; LeBoeuf, D.; Chang, J.; Ramshaw, B. J.; et al. Direct Measurement of the Upper Critical Feld in Cuprate Superconductors. *Nat. Commun.* **2014**, *5*, 1−8.

(2) Kenfaui, D.; Sibeud, P.-F.; Louradour, E.; Noudem, J. G.; Chaud, X. High Trapped Field Performances in Thin-Wall YBCO Bulk Cryomagnets. *Appl. Phys. Lett.* **2013**, *102*, 202602−202606.

(3) Durrell, J. H.; Dennis, A. R.; Jaroszynski, J.; Ainslie, M. D.; Palmer, K. G. B.; Shi, Y.-H.; Campbell, A. M.; Hull, J.; Strasik, M.; Hellstrom, E. E.; et al. A Trapped Feld of 17.6 T in Melt-Processed Bulk Gd-Ba-Cu-O Reinforced with Shrink-Fit Steel. *Supercond. Sci. Technol.* **2014**, *27*, 082001−082005.

(4) Krabbes, G.; Fuchs, G.; Canders, W.-R.; May, H.; Palka, R. *High Temperature Superconductor Bulk Material: Fundamentals, Processing, Properties Control, Application Aspects*; WILEY-VCH Verlag GmbH & Co. KGaA: Weinheim, Germany, 2006.

(5) Babu, N. H.; Shi, Y.; Iida, K.; Cardwell, D. A. A Practical Route for the Fabrication of Large Single-Crystal (RE)−Ba−Cu−O Superconductors. *Nat. Mater.* **2005**, *4*, 476−480.

(6) Fuchs, G.; Krabbes, G.; Müller, K.-H.; Verges, P.; Schultz, L.; Gonzalez-Arrabal, M.; Eisterer, R.; Weber, H. W. High Magnetic Fields in Superconducting Permanent Magnets. *J. Low Temp. Phys.* **2003**, *133*, 159−179.

(7) Tomita, M.; Murakami, M. High-Temperature Superconductor Bulk Magnets that Can Trap Magnetic Fields of over 17 T at 29 K. *Nature* **2003**, *421*, 517−520.

(8) Fuchs, G.; Schatzle, P.; Krabbes, G.; Gruß, S.; Verges, P.; Muller, K.-H.; Fink, J.; Schultz, L. Trapped Magnetic Fields Larger than 14 T in Bulk $YBa_2Cu_3O_{7-x}$. *Appl. Phys. Lett.* **2000**, *76*, 2107−2109.

DOI: 10.1021/acs.jpclett.5b00906
J. Phys. Chem. Lett. 2015, 6, 2999−3005

(9) Gruss, S.; Fuchs, G.; Krabbes, G.; Verges, P.; Stöver, G.; Müller, K.-H.; Fink, J.; Schultz, L. Superconducting Bulk Magnets: Very High Trapped Fields and Cracking. *Appl. Phys. Lett.* **2001**, *79*, 3131−3134.
(10) Campbell, A. M.; Cardwell, D. A. Bulk High Temperature Superconductors for Magnet Applications. *Cryogenics* **1997**, *37*, 567−575.
(11) Bean, C. P. Magnetization of High-field Superconductors. *Phys. Rev. Lett.* **1962**, *8*, 250−253.
(12) Kenfaui, D.; Chaud, X.; Hai, X.; Louradour, E.; Noudem, J. G. Thin-Wall YBCO Single Domains Oxygenated under Pressure: Optimization of Trapping Properties. *IEEE trans. Appl. Supercond.* **2013**, *23*, 7201005−7201009.
(13) Sakai, N.; Ishihara, D.; Inoue, I.; Murakami, M. Formation of Pores in Melt-Processed RE-Ba-Cu-O and the Techniques to Reduce Pore Density. *Supercond. Sci. Technol.* **2002**, *15*, 698−701.
(14) Specht, E. D.; Sparks, C. J.; Dhere, A. G.; Brynestad, J.; Cavin, O. B.; Kroeger, D. M.; Oye, H. A. Effect of Oxygen Pressure on the Orthorhombic-Tetragonal Transition in the High-Temperature Superconductor $YBa_2Cu_3O_x$. *Phys. Rev. B: Condens. Matter Mater. Phys.* **1988**, *37*, 7426−7434.
(15) Wang, W.; Peng, B.; Chen, Y.; Guo, L.; Cui, X.; Rao, Q.; Yao, X. Effective Approach to Prepare Well c-Axis-Oriented YBCO Crystal by Top-Seeded Melt-Growth. *Cryst. Growth Des.* **2014**, *14* (5), 2302−2306.
(16) Devendra Kumar, N.; Shi, Y.; Zhai, W.; Dennis, A. R.; Durrell, J. H.; Cardwell, D. A. Buffer Pellets for High-Yield, Top-Seeded Melt Growth of Large Grain Y−Ba−Cu−O Superconductors. *Cryst. Growth Des.* **2015**, *15* (3), 1472−1480.
(17) Li, H.; Fan, W.; Peng, B.; Wang, W.; Zhuang, Y.; Guo, L.; Yao, X.; Ikuta, H. Seed-Size Effect on the Growth and Superconducting Performance of YBCO Single-Grain Bulks. *Cryst. Growth Des.* **2015**, *15* (4), 1740−1744.
(18) Yang, W.; Guo, X.; Wan, F.; Li, G. Real-Time Observation and Analysis of Single-Domain YBCO Bulk Superconductor by TSIG Process. *Cryst. Growth Des.* **2011**, *11* (7), 3056−3059.
(19) Isfort, D.; Chaud, X.; Tournier, R.; Kapelski, G. Cracking and Oxygenation of YBaCuO Bulk Superconductors: Application to c-Axis Elements for Current Limitation. *Phys. C* **2003**, *390*, 341−355.
(20) Klaser, M.; Kaiser, J.; Stock, F.; Muller-Vogt, G.; Erb, A. Comparative Study of Oxygen Diffusion in Rare Earth $REBa_2Cu_3O_{7-\delta}$ Single Crystals (RE=Y, Er, Dy) with Different Impurity Levels. *Phys. C* **1998**, *306*, 188−198.
(21) Rothman, S. J.; Routbort, J. L.; Welp, U.; Baker, J. E. Anisotropy of Oxygen Tracer Diffusion in Single-Crystal $YBa_2Cu_3O_{7-\delta}$. *Phys. Rev. B: Condens. Matter Mater. Phys.* **1991**, *44*, 2326−2333.
(22) Sakai, N.; Seo, S. J.; Inoue, K.; Miyamoto, T.; Murakami, M. *In Advances in Superconductivity XI*; Springer: Tokyo, 1999.
(23) Touloukian, Y. S.; Powell, R. W.; Ho, C. Y.; Klemens, P. G. *Thermophysical Properties of Matter, V. 1: Thermal Conductivity - Metallic Elements and Alloys*; IFI/Plenum: New York/Washington, 1970.
(24) Lykov, A. N. Magnetic Flux Creep in HTSC and Anderson-Kim Theory. *Low Temp. Phys.* **2014**, *40*, 773−795.
(25) Wachtman, J. B. *Mechanical Properties of Ceramics*; Wiley and Sons, Inc.: New York, 1996.
(26) Tancret, F.; Monot, I.; Osterstock, F. Toughness and Thermal Shock Resistance of $YBa_2Cu_3O_{7-x}$ Composite Superconductors Containing Y_2BaCuO_5 or Ag Particles. *Mater. Sci. Eng., A* **2001**, *298*, 268−283.
(27) Joo, J.; Jung, S.-B.; Nah, W.; Kim, J.-Y.; Kim, T. S. Effects of Silver Additions on the Mechanical Properties and Resistance to Thermal Shock of $YBa_2Cu_3O_{7-x}$ Superconductors. *Cryogenics* **1999**, *39*, 107−113.
(28) Irwin, G. Analysis of Stress and Strain Near the End of a Crack Traversing a Plate. *J. Appl. Mech.* **1957**, *24*, 361−364.
(29) Collings, E. W.; Sumption, M. D. *In Advances in Superconductivity VII*; T. Springer: Tokyo, 1995.

DOI: 10.1021/acs.jpclett.5b00906
J. Phys. Chem. Lett. 2015, 6, 2999−3005